Development of Three Dimensional Two Phase Flow Model for the SPACE code

Chan Eok Park, Myung Taek Oh, Sang Yong Lee, and Shin Whan Kim*
KEPCO E&C Company, Inc., 1045 Daedeok-daero, Yuseong-gu, Daejeon, 305-353
**Corresponding author:cepark@kepco-enc.com*

1. Introduction

Staggered mesh semi-implicit numerical scheme in the SPACE code has been developed to have capability of dealing with 1-D or 3-D two phase flow in Cartesian and cylindrical mesh system[1-2]. In this paper, the flexible feature of the staggered mesh system of SPACE will be described, focusing on how to model the complex geometries and various types of their connections typically encountered in nuclear power plant systems. The semi-implicit numerical solution scheme using the staggered mesh system and some of the application results will be also presented.

2. Multi-dimensional staggered mesh system

2. 1 Mesh system

Fig. 1 shows the staggered mesh used in the SPACE code. All of the geometric quantities are described in terms of cell volume, centroid, face area, and face center, so that Cartesian and cylindrical mesh systems can be simultaneously operated in this mesh system. Each scalar cell has normally six faces in 3-D Cartesian or cylindrical mesh blocks. But 2-D Cartesian meshes or 1-D pipe can be also represented only by reducing the number of the surrounding faces. Direction of the cell and the associated faces can be distinguished by the unique number sequentially given to each face. Each momentum cell is shifted by the half size of scalar cell. Hence, it consists of the front half part of the owner scalar cell and the back half part of the neighbor scalar cell. Each face can be divided into several sub-faces. With these sub-faces, one-dimensional or three-dimensional branches are easily modeled. Generally curved pipes can be also represented by providing inclined and azimuthal angles to each scalar cell.

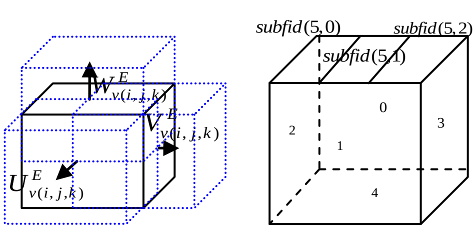

Fig. 1 SPACE staggered mesh system

2. 2 Mesh generation and system construction

Unless the branch or cross-flow typed sub-faces are used, the hexahedral staggered meshes have similar features to a structural mesh system. Therefore, the simple mesh blocks can be easily generated on an algebraic basis. The SPACE code provides a simple way to construct various types of mesh blocks, such as three-dimensional Cartesian, cylindrical blocks, one-dimensional cell, face, pipe, branch, and so on. It also provides a methodology to construct complex systems by connecting the already generated mesh blocks with the block linkage data given by users.

As a result, the SPACE staggered mesh system allows users to easily model 1D branch, generally curved pipe , 1D cross flow, 3D Cartesian and cylindrical blocks, 3D branch, 1D/3D interface with or without momentum direction change(see Fig. 2).

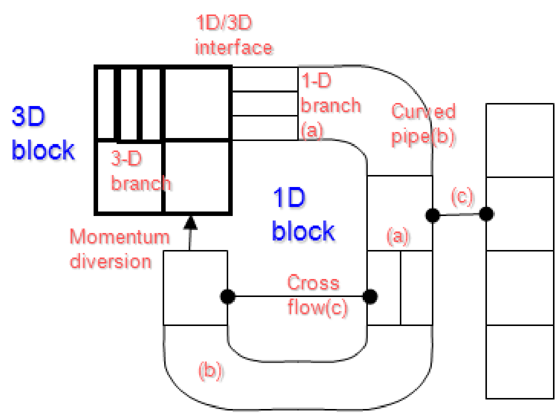

Fig. 2 System construction using SPACE staggered mesh

3. Numerical solution scheme

3.1 Discretized equations

By applying Finite Volume Method(FVM), the ten governing equations of SPACE, which consist of three field mass, momentum, energy equations and a continuity equation of non-condensable gas mixture, can be expressed as follows.

- Continuity equation

$$\varepsilon V_P \frac{\alpha_g^n \rho_n^n - \alpha_g \rho_n}{\Delta t} + \sum_{E\in P} \varepsilon^E \, {}^d\alpha_g^E \, {}^d\rho_n^E \left(\iota_P^E U_{gn}^n A^E \right) = 0 \quad (1)$$

$$\begin{aligned} &\varepsilon V_P \frac{\alpha_g^n \rho_v^n - \alpha_g \rho_v}{\Delta t} + \sum_{E\in P} \varepsilon^E \, {}^d\alpha_g^E \, {}^d\rho_v^E \left(\iota_P^E U_{gn}^n A^E \right) \\ &= \varepsilon V_P \left(\Gamma_l^n + \Gamma_d^n + \Gamma_l^w + \Gamma_d^w \right) \end{aligned} \quad (2)$$

$$\begin{aligned} &\varepsilon V_P \frac{\alpha_d^n \rho_d^n - \alpha_d \rho_d}{\Delta t} + \sum_{E\in P} \varepsilon^E \, {}^d\alpha_d^E \, {}^d\rho_d^E \left(\iota_P^E U_{dn}^n A^E \right) \\ &= \varepsilon V_P \left(-\Gamma_d^n - \Gamma_d^w + S_E - S_D \right) \end{aligned} \quad (3)$$

$$\begin{aligned} &\varepsilon V_P \frac{\alpha_l^n \rho_l^n - \alpha_l \rho_l}{\Delta t} + \sum_{E\in P} \varepsilon^E \, {}^d\alpha_l^E \, {}^d\rho_l^E \left(\iota_P^E U_{ln}^n A^E \right) \\ &= \varepsilon V_P \left(-\Gamma_l^n - \Gamma_l^w - S_E + S_D \right) \end{aligned} \quad (4)$$

- Energy equation

$$\begin{aligned} &\varepsilon V_P \frac{\alpha_g^n \left(\rho_v^n e_v^n + \rho_n^n e_n^n \right) - \alpha_g \left(\rho_v e_v + \rho_n e_n \right)}{\Delta t} \\ &+ \sum_{E\in P} \iota_P^E \varepsilon^E \, {}^d\alpha_g^E \left({}^d\rho_v^E \, {}^d e_v^E + {}^d\rho_n^E \, {}^d e_n^E \right) \left(U_{gn}^n A^E \right) \\ &+ P \sum_{E\in P} \iota_P^E \varepsilon^E \, {}^d\alpha_g^E U_{gn}^n A^E \\ &= \varepsilon V_P \left[-P \frac{\alpha_g^n - \alpha_g}{\Delta t} + Q_{iv-l}^n + \Gamma_l^n h_{vl}^* + \Gamma_d^n h_{vd}^* + Q_{iv-d}^n \right] \\ &+ \varepsilon V_P \left(Q_g^w + \Gamma_l^w h_{vl}' + Q_{iv-l}^w + \Gamma_d^w h_{vd}' + Q_{iv-d}^w + Q_{l-n}^n + Q_{d-n}^n \right) \end{aligned} \quad (5)$$

$$\begin{aligned} &\varepsilon V_P \frac{\alpha_d^n \rho_d^n e_d^n - \alpha_d \rho_d e_d}{\Delta t} + \sum_{E\in P} \iota_P^E \varepsilon^E \, {}^d\alpha_d^E \, {}^d\rho_d^E \, {}^d e_d^E \left(U_{dn}^n A^E \right) \\ &+ P \sum_{E\in P} \iota_P^E \varepsilon^E \, {}^d\alpha_d^E U_{dn}^n A^E \\ &= \varepsilon V_P \left[-P \frac{\alpha_d^n - \alpha_d}{\Delta t} + Q_{id}^n - \Gamma_d^n h_d^* + S_E h_l - S_D h_d - Q_{d-n}^n \right] \\ &+ \varepsilon V_P \left(Q_d^w - \Gamma_d^w h_d' + Q_{id}^w \right) \end{aligned} \quad (6)$$

$$\begin{aligned} &\varepsilon V_P \frac{\alpha_l^n \rho_l^n e_l^n - \alpha_l \rho_l e_l}{\Delta t} + \sum_{E\in P} \iota_P^E \varepsilon^E \, {}^d\alpha_l^E \, {}^d\rho_l^E \, {}^d e_l^E \left(U_{ln}^n A^E \right) \\ &+ P \sum_{E\in P} \iota_P^E \varepsilon^E \, {}^d\alpha_l^E U_{ln}^n A^E \\ &= \varepsilon V_P \left[-P \frac{\alpha_l^n - \alpha_l}{\Delta t} + Q_{il}^n - \Gamma_l^n h_l^* - S_E h_l + S_D h_d - Q_{l-n}^n \right] \\ &+ \varepsilon V_P \left(Q_l^w - \Gamma_l^w h_l' + Q_{il}^w \right) \end{aligned} \quad (7)$$

- Momentum equation

In the hexahedral shape of a scalar cell, each orthogonal face can be categorized into three different types, depending on the direction of the face vector. The components of the cell velocity vector, $U_{(k)}$, are calculated by averaging the same type face velocities. If the transverse direction velocity is denoted by $XU_{(k)}$ at each face, the momentum equation can be expressed as follows.

$$\begin{aligned} &\varepsilon^E V^E \frac{\left(U_{gn}^E \right)^n - U_{gn}^E}{\Delta t} \\ &+ \varepsilon_{(k=\text{face type of } E)}^{Neighbor} \, {}^d U_{g(k)}^{Neighbor} \left(A_{(k)}^{Neighbor} U_{g(k)}^{Neighbor} \right) \\ &- \varepsilon_{(k)}^{Owner} \, {}^d U_{g(k)}^{Owner} \left(A_{(k)}^{Owner} U_{g(k)}^{Owner} \right) \\ &+ \sum_{E' \in Owner, typ \neq k} \varepsilon^{E'} \, {}^d XU_{g(k)}^{Fhcell} \left(\iota_{Owner}^{E'} \frac{1}{2} U_{gn}^{E'} A^{E'} \right) \\ &+ \sum_{E' \in Neighbor, typ \neq k} \varepsilon^{E'} \, {}^d XU_{g(k)}^{Bhcell} \left(\iota_{Neighbor}^{E'} \frac{1}{2} U_{gn}^{E'} A^{E'} \right) \\ &+ F_{g(k)} V^E - \; U_{gn}^E \varepsilon_{(k)}^{Neighbor} \left(A_{(k)}^{Neighbor} U_{g(k)}^{Neighbor} \right) \\ &+ U_{gn}^E \varepsilon_{(k)}^{Owner} \left(A_{(k)}^{Owner} U_{g(k)}^{Owner} \right) \\ &- U_{gn}^E \sum_{E' \in Owner, typ \neq k} \varepsilon^{E'} \left(\iota_{Owner}^{E'} \frac{1}{2} U_{gn}^{E'} A^{E'} \right) \\ &- U_{gn}^E \sum_{E' \in Neighbor, typ \neq k} \varepsilon^{E'} \left(\iota_{Neighbor}^{E'} \frac{1}{2} U_{gn}^{E'} A^{E'} \right) \\ &= \frac{1}{\rho_g} \varepsilon^E A^E \left(P_{Owner}^n - P_{Neighbor}^n \right) + \varepsilon^E V^E \mathbf{B} \cdot \mathbf{n}^E + Other \ sources \end{aligned}$$

(8)

$$
\begin{aligned}
&\varepsilon^E V^E \frac{\left(U_{dn}^E\right)^n - U_{dn}^E}{\Delta t} \\
&+\varepsilon_{(k=face\ type\ of\ E)}^{Neighbor}\ {}^{d}U_{d(k)}^{Neighbor}\left(A_{(k)}^{Neighbor}U_{d(k)}^{Neighbor}\right) \\
&-\varepsilon_{(k)}^{Owner}\ {}^{d}U_{d(k)}^{Owner}\left(A_{(k)}^{Owner}U_{d(k)}^{Owner}\right) \\
&+\sum_{E'\in Owner, typ\neq k} \varepsilon^{E'}\ {}^{d}XU_{d(k)}^{Fhcell}(\iota_{Owner}^{E'}\frac{1}{2}U_{dn}^{E'}A^{E'}) \\
&+\sum_{E'\in Neighbor, typ\neq k} \varepsilon^{E'}\ {}^{d}XU_{d(k)}^{Bhcell}(\iota_{Neighbor}^{E'}\frac{1}{2}U_{dn}^{E'}A^{E'}) \\
&+F_{d(k)}V^E - \ U_{dn}^E\varepsilon_{(k)}^{Neighbor}\left(A_{(k)}^{Neighbor}U_{d(k)}^{Neighbor}\right) \\
&+U_{dn}^E\varepsilon_{(k)}^{Owner}\left(A_{(k)}^{Owner}U_{d(k)}^{Owner}\right) \\
&-U_{dn}^E\sum_{E'\in Owner, typ\neq k} \varepsilon^{E'}(\iota_{Owner}^{E'}\frac{1}{2}U_{dn}^{E'}A^{E'}) \\
&-U_{dn}^{E'}\sum_{E\in Neighbor, typ\neq k} \varepsilon^{E'}(\iota_{Neighbor}^{E'}\frac{1}{2}U_{dn}^{E'}A^{E'}) \\
&=\frac{1}{\rho_d}\varepsilon^E A^E(P_{Owner}^n - P_{Neighbor}^n) + \varepsilon^E V^E \mathbf{B}\cdot\mathbf{n}^E + Orther\ sources
\end{aligned}
\tag{9}
$$

$$
\begin{aligned}
&\varepsilon^E V^E \frac{\left(U_{ln}^E\right)^n - U_{ln}^E}{\Delta t} \\
&+\varepsilon_{(k=face\ type\ of\ E)}^{Neighbor}\ {}^{d}U_{l(k)}^{Neighbor}\left(A_{(k)}^{Neighbor}U_{l(k)}^{Neighbor}\right) \\
&-\varepsilon_{(k)}^{Owner}\ {}^{d}U_{l(k)}^{Owner}\left(A_{(k)}^{Owner}U_{l(k)}^{Owner}\right) \\
&+\sum_{E'\in Owner, typ\neq k} \varepsilon^{E'}\ {}^{d}XU_{l(k)}^{Fhcell}(\iota_{Owner}^{E'}\frac{1}{2}U_{ln}^{E'}A^{E'}) \\
&+\sum_{E'\in Neighbor, typ\neq k} \varepsilon^{E'}\ {}^{d}XU_{l(k)}^{Bhcell}(\iota_{Neighbor}^{E'}\frac{1}{2}U_{ln}^{E'}A^{E'}) \\
&+F_{l(k)}V^E - \ U_{ln}^E\varepsilon_{(k)}^{Neighbor}\left(A_{(k)}^{Neighbor}U_{l(k)}^{Neighbor}\right) \\
&+U_{ln}^E\varepsilon_{(k)}^{Owner}\left(A_{(k)}^{Owner}U_{l(k)}^{Owner}\right) \\
&-U_{ln}^E\sum_{E'\in Owner, typ\neq k} \varepsilon^{E'}(\iota_{Owner}^{E'}\frac{1}{2}U_{ln}^{E'}A^{E'}) \\
&-U_{ln}^{E}\sum_{E'\in Neighbor, typ\neq k} \varepsilon^{E'}(\iota_{Neighbor}^{E'}\frac{1}{2}U_{ln}^{E'}A^{E'}) \\
&=\frac{1}{\rho_l}\varepsilon^E A^E(P_{Owner}^n - P_{Neighbor}^n) + \varepsilon^E V^E \mathbf{B}\cdot\mathbf{n}^E + Orther\ sources
\end{aligned}
\tag{10}
$$

where the source terms, $F_{\phi(k)}$, representing the centrifugal and Coriolis force are:

$$
\begin{aligned}
&Cartesian\ coordinate(x,y,z:U_x,U_y,U_z): \\
&F_{\phi(1)}=0,\quad F_{\phi(2)}=0,\quad F_{\phi(3)}=0
\end{aligned}
\tag{11}
$$

$$
\begin{aligned}
&Cylindrical\ coordinate(r,\theta,z:U_r,U_\theta,U_z): \\
&F_{\phi(1)}=-\frac{U_{\phi(2)}^2}{r},\quad F_{\phi(2)}=\frac{U_{\phi(1)}U_{\phi(2)}}{r},\quad F_{\phi(3)}=0
\end{aligned}
\tag{12}
$$

In the above discretized equations, the following notations are used.

Q_{ild} : heat transfer rate per unit volume between droplet-gas interface
$Q_{il\,l}$: heat transfer quantity per unit volume in between continuous liquid-gas
Q_{ill} : heat transfer quantity per unit volume in between continuous liquid-gas
Q_{ivd} : heat transfer quantity per unit volume in between droplet-gas
$Q_{iv\,l}$: heat transfer quantity per unit volume in between continuous liquid-gas interfacial area and gas
Q_{wk} : heat transfer quantity from wallside to each phase
S_D : droplet departure rate per unit volume
S_E : droplet adhesion rate per unit volume
U: Velocity
V: Volume
XU: cross direction velocity
ε : porosity
Γ : vapor generation rate per unit volume, phase change rate per unit volume

The superscripts and subscripts are also used as follows.

d: droplet
E: face property
g: vapor/gas mixture
k: face type(direction)
l: continuous liquid
n: normal direction(subscript)
n: new time(superscript)
p: present cell
w: wall

3.2 Time advancement scheme

In the semi-Implicit scheme, the convection terms of momentum equations are discretized in the explicit manner, while the pressure gradient terms are implicitly treated. The system pressure matrix can be derived by substituting the linear relationship between velocity and pressure gradient into the implicit velocity terms of mass and energy conservation equations, and inverting the cell matrix. After the system pressure matrix is solved, the solutions for other primitive variables are obtained by the back substitution.

4. Test results

4.1 Nodalization of a typical PWR

Fig. 3 shows an example of nodalization for Nuclear Steam Supply System(NSSS) of a typical PWR. It consists of a combination of one dimensional flow network, three dimensional Cartesian, and cylindrical mesh blocks. Cartesian type block meshes are used for modeling the reactor core, lower and upper plenum, and reactor vessel heads. The downcomer annulus is modeled by a cylindrical mesh blocks. The hot leg and cold legs, pressurizer, surge line, Steam generator(SG) U-tubes, and the flow network at the secondary side of SG are also constructed by one-dimensional mesh blocks.

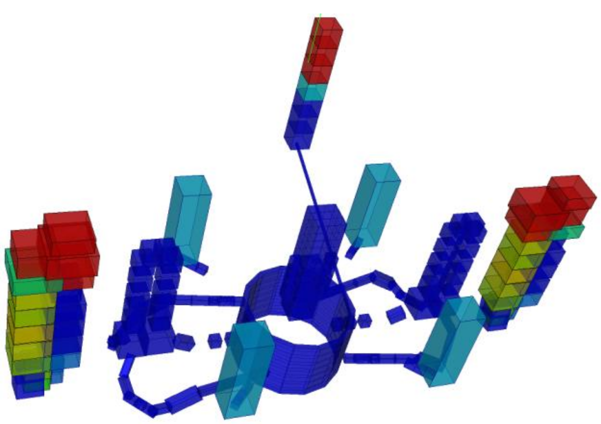

Figure 3 Nodalization for NSSS system of a typical PWR

4.2 Blowdown and reflood test

A simplified test for blowdown and reflood phenomena during a cold leg break LOCA are performed with the above nodalization of a typical PWR. Before the simplified LOCA test, null-transient calculation is carried out to obtain full power steady state of APR1400. Double-ended guillotine break occurs at time zero, and the reactor coolant system experiences blowdown and reflood phases. Fig. 4 shows the distribution of void fraction after quenching time of the reflood phase. The overall system thermal hydraulic behavior during blowdown and reflood phases are found to be quite reasonable.

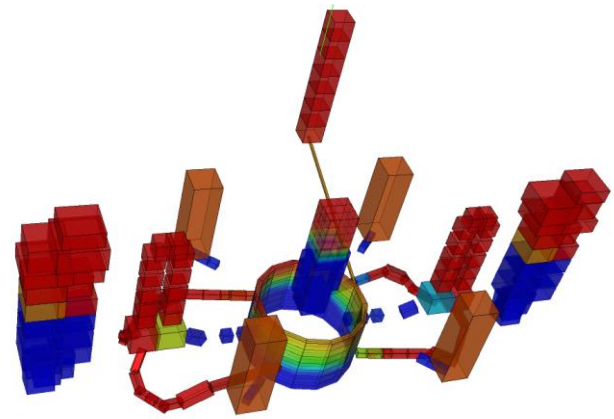

Figure 4 Distribution of void fraction at 200 seconds.

5. Conclusion

In this paper, nodalization capability of the staggered mesh system of SPACE is demonstrated. The SPACE staggered mesh system is useful to combine three-dimensional Cartesian, cylindrical mesh blocks, one-dimensional curved pipes, branches, and cross-flow junctions. The connection technique between different types of mesh blocks are also found to work properly. Finally, the simplified blowdown and reflood test for a typical PWR shows that the semi-implicit numerical scheme works properly with the flexible staggered mesh system of SPACE.

Acknowledgment

This work was supported by Nuclear R&D Program of the Korea Institute of Energy Technology and Planning grant funded by the Korean government.

REFERENCES

[1] C. E. Park, “A Two-Fluid, Three-Field Hydraulic Solver for the Safety Analysis Code, SPACE”, ANS winter meeting, Nov. 2009

[2] S. J. Ha, C. E. Park, K. D. Kim, and C. H. Ban, “Development of the SPACE Code for Nuclear Power Plants”, Nuclear Technology, Vol. 43, No. 1, 2011.